Heliyon 10 (2024) e31264

Contents lists available at ScienceDirect

Heliyon

journal homepage: www.cell.com/heliyon

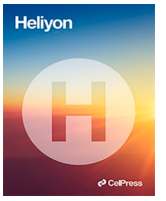

Research article

Gasification chars and activated carbon: Systematic physico-chemical characterization and effect on biogas production

Christian Margreiter [a,b], Maraike Probst [a], Eva Maria Prem [a], Angela Hofmann [b], Andreas Otto Wagner [a,*]

[a] Department of Microbiology, Universität Innsbruck, Technikerstraße 25d, A-6020, Innsbruck, Austria
[b] Josef Ressel Center for the Production of Activated Carbon from Municipal Residues, MCI Innsbruck, Maximilianstraße 2, A-6020, Innsbruck, Austria

ARTICLE INFO

Keywords:
Activated carbons
Gasification char
Anaerobic digestion
Biogas production
Sewage sludge
Biochar

ABSTRACT

Gasification residues/chars (GR) and activated carbon (AC) are added to wastewater treatment processes mainly as a fourth purification stage, e.g., to adsorb heavy metals or pharmaceutical residues. However, the effects of GR or AC, which are transferred to the anaerobic digestion (AD) via the sludge, are not yet fully understood. Although, the positive effect of char addition on AD has been demonstrated in several investigations, systematic studies with chemically well described chars are still missing. Therefore, in this study, different chars were characterized in detail, subjected to AD in different concentrations, and their effect on methane production investigated. GR of a gasification plant with a floating fixed bed technology, carbon made by chemical impregnation with $ZnCl_2$ from waste-wood, carbon produced by thermochemical activation with CO_2 from GR and commercial powdered AC were used for the experiments. Among others, thermogravimetric analysis, physisorption, pH, and conductivity analysis were used to characterize the chars. Mesophilic AD batch tests with different concentrations (0.025, 0.05, 0.5, 1.0, 7.0, 14.0 gL^{-1}) of all chars (GR and ACs, respectively) were performed with digester sludge from a wastewater treatment plant for a period of 47 d. Volatile fatty acids (VFA) as well as biogas production and CH_4 concentrations were monitored. It could be shown, that concentrations below 1.0 g char L^{-1} did not result in significant effects on CH_4 and/or VFA production, whereas high concentrations of GR and AC influenced both, the CH_4 yield and kinetics. Depending on the production process and the characteristics of the chars, the effect on AD varied, whereby both, positive and negative effects on biogas yield and methane production were observed. This study provides the first systematic evaluation of char application to AD processes, and therefore allows for better predictions of char applicability and effect.

1. Introduction

In biogas plants, organic substrates, e.g. waste water and waste water sludge, are converted into energy via anaerobic digestion (AD) [1]. More precisely, in AD, microorganisms convert biodegradable material into biogas (mainly CH_4 and CO_2), which is a

* Corresponding author.
E-mail addresses: Christian.Margreiter@student.uibk.ac.at (C. Margreiter), maraike.probst@uibk.ac.at (M. Probst), eva.prem@uibk.ac.at (E.M. Prem), Angela.Hofmann@mci.edu (A. Hofmann), andreas.wagner@uibk.ac.at (A.O. Wagner).

https://doi.org/10.1016/j.heliyon.2024.e31264
Received 26 January 2024; Received in revised form 29 April 2024; Accepted 14 May 2024
Available online 14 May 2024

renewable energy source. The increase in energy production from 6 200 GWh in 2009 to 18 012 GWh in 2019 clearly shows the growing economic interest in biogas production in Europe [2]. However, there are still unanswered scientific questions, whose investigation will help understanding and optimizing AD.

The use of carbonaceous materials, such as char produced from biomass by various thermochemical processes can improve the efficiency of biogas plants [3]. Char types, such as biochar, activated carbon (AC), and gasification residues/chars (GR), differ in their properties, due to different feedstocks and production processes Previous studies reported a positive effect of biochar on biogas production, with increased CH_4 production by up to 34 % [4,5]. The positive effects of biochar on AD were primarily attributed to its porous structure, which may promote biofilm formation and thus syntrophication [6], ion exchange [7], buffering capacity [5], and ammonium migration inhibition [5,8].

AC has been specifically designed and manufactured for the removal of all types of contaminants. The removal is based on high adsorption capacities due to the high specific surface area (SSA), which is achieved through porous structures. The high SSA can reach up to 3 000 $m^2\ g^{-1}$ [9]. Few studies applied AC to AD and most of them showed a positive effect of AC addition [10,11]. Only one study reported a negative effect of AC on CH_4 production [12]. The positive effect of AC was mainly attributed to its ability of adsorbing substances that negatively impact microorganisms, such as active pharmaceutical ingredients like antibiotics [13], and the high electrical conductivity of the char, which is considered to improve direct interspecies electron transfer (DIET) [14,15]. A negative impact might be that not only inhibitors but also substrates, such as volatile fatty acids (VFAs), can be adsorbed. Lower substrate availability may result in lower microbial metabolization [10], and consequently in a decreased chemical oxygen demand (COD) in AD system applying AC [15,16].

GR are a by-product of gasification processes, which primarily use biomass to produce energy [17]. Research on the use of GR in AD studies is, to our knowledge, limited. However, two notable studies have shown promising results with the use of GR to mitigate ammonium inhibition through the immobilization of ammonium tolerant methanogens on GR [18,19]. Being a residue, GR could be a sustainable additive for AD improvement [20].

Most studies reporting a positive effect of char on AD neither give a clear definition of the char's type and characteristics, nor apply biochar produced specifically for a given AD process. Moreover, studies usually test a single char without offering a comparison among chars. Such comparison is relevant though, because feedstock and production processes have a significant influence on char properties [3], which might affect AD.

Due to the lack of systematic studies, currently neither the char properties promoting biogas production nor the reasons for char effects on AD processes can be concluded. Therefore, this study focused on characterizing different types of char, which were then used for AD under controlled lab conditions to understand the effect of char properties on AD. For this purpose, mesophilic batch experiments applying sewage sludge as an inoculum were carried out and different types of char were added. The four types of carbon used in this study were GR made from recycled waste material, CO_2 AC made from GR, and chemically activated carbon from wood with $ZnCl_2$. A commercially available powdered activated carbon served as a reference.

2. Material and methods

2.1. Experimental design

After production the chars were characterized by scanning electron microscopy (SEM), pH and EC measurements, elemental analysis (ICP), thermogravimetric analysis (TGA), gas adsorption analysis, carbon leaching tests, and volatile fatty acid adsorption experiments. Subsequently, chars were used for AD in batch experiments.

2.2. Chars

The GR used was a by-product of the wood gasification process. It was produced in a fixed-bed floating reactor developed by SynCraft and operated by the Innsbrucker Kommunalbetriebe "IKB" at the WWTP Innsbruck/Rossau, Austria [21]. The raw material for the production of IKB char was residual forest wood consisting mainly of sapwood, bark, tops, and branches. The GR was provided by the "Innsbrucker Kommunalbetriebe". CO_2 AC was produced by activating GR using CO_2. A laboratory scale fluidised bed reactor was used to activate the GR (850 °C, 20min (2 L min^{-1})). "Carbopal AP Supra" (Com AC) was purchased from the company Donau Carbon (Germany). Waste wood from the local waste wood plant, classified under waste code SN 17201, was used for activation using $ZnCl_2$ according to Ref. [22] (500 °C; 2 h; 10 °C min^{-1}; 5:1).

GR and ACs were dried at 105 °C overnight. All chars except Com AC were grounded and sieved to 1 mm to have a defined size. The CH_4 production should not be affected by different particle sizes up to 3 mm according to Ref. [23].

2.3. Characterization of the chars

NeoScope JCM-5000 SEM (JOEL) was used to visualize the structure of all chars before and during the batch experiment. Sludge samples were analyzed on day 35 after lyophilization using a Mitsubishi GOT10000 VaCo2-II. Reverse osmosis (RO) water and 10 % (w/v) char were used to assess the pH and electrical conductivity (EC) of the chars using a pH/Cond 3320 pH/EC meter (WTW, Germany) after shaking for 1 h. Optical Emission Spectrometry (OES) combined with Inductively Coupled Plasma (ICP-OES, acid fusion with HNO_3, Spectro Genesis, SPECTRO Analytical Instruments GmbH) was used for elemental analysis of all chars. To determine the moisture content, the volatile solids-, fixed carbon- and the ash content of the ACs a thermogravimetric analysis was carried out

with 15.0 g char using a TGA analyzer (Netzsch, STA449 F5 Jupiter, Germany) with setting depicted in Table 1.

The mass loss [%] of the samples was calculated following equations (1)–(4).

$$w_{H2O} = \frac{m_{wet} - m_{dry}}{m_{wet}} \tag{1}$$

$$w_{VM} = \frac{m_{VM}}{m_{dry}} \tag{2}$$

$$w_{FC} = 1 - w_{VM} - w_{ash} \tag{3}$$

$$w_{ash} = \frac{m_{ash}}{m_{dry}} \tag{4}$$

whereby

w_{H2O} is the mass water content
w_{VM} is the mass volatile matter
w_{FC} is the mass of fixed carbon
w_{ash} is the mass of the ash content

Gas adsorption analysis with N_2 was carried out to characterize the structural properties of the chars. The specific surface area (SSA) of the chars was calculated using the Brunauer-Emmett-Teller (BET) isotherm theory. Prior to analysis, 100–150 mg of each AC sample was degassed (VacPrep 061, Micromeritics) at 200 °C for 12 h. The chars were then set under an atmosphere of N_2 at 77 K using a 3Flex (Micromeritics) apparatus and their adsorption/desorption isotherms were recorded at 60–80 points with an equilibrium time of 10 s. Surface areas were calculated using a linearized form of the BET isotherm equation according to equation (5).

$$\frac{1}{V_{Ads} \bullet \left(\frac{p^*}{p} - 1\right)} = \frac{c-1}{c \bullet V_{Ads}} \bullet \frac{p}{p^*} + \frac{1}{c \bullet V} \tag{5}$$

whereby

V_M is the monolayer volume,
V_{Ads} is the total adsorbed volume,
c is the BET constant [24],
p is the pressure,
p^* the saturation pressure.

The pressure difference resulting from N_2 adsorption was used to calculate the V_{Ads} volume. The adsorbed amount of material required for a monolayer was calculated assuming an ideal gas. The SSA was obtained by multiplying the cross-sectional area of an N_2 molecule by the number of N_2 molecules (amount of substance [$gmol^{-1}$] • Avogadro's constant) based on the resulting amount of N_2 adsorbed.

The biological oxygen demand (BOD) of the GR, CO_2 AC and Com AC was determined because of their high carbon leaching potential (see COD data 3.3) using 14.0 g char L^{-1} water according to the WTW operating manual IS6 [25]. The BOD-bottles with manometer (WTW, Germany) were incubated for 5 d at 20 °C in a BOD Oxitop incubator (WTW, Germany). Carbon leaching COD was determined using Nanocolor cuvette tests (Macherey&Nagel, Germany) after 24 h applying 14.0 g carbon L^{-1} water. A Dionex™ Aquion™ ion chromatography (IC) system (Thermo Fisher Scientific, Germany) was used to determine the anion- (Na, K, Mg, Ca) and cation- (F^-, Cl^-, $[SO_4]^{2-}$, PO_4^{3-}) concentration leached from the chars (GR, CO_2 AC and Com AC). Anion and cation determinations were performed using methods described in the Dionex™ IonPac™ CS12A and IonPac™ AS14A IC column operating manuals [26,27]. Because the Zn^{2+} concentration was too high for the ion chromatograph, the carbon leaching of $ZnCl_2$ AC was obtained using a Nanocolor photometric cuvette test (Macherey&Nagel, Germany) according to the manufacturer's recommendations.

As tars are produced during the thermochemical conversion of biomass to char, the carbon leaching of Polycyclic aromatic

Table 1
TGA temperature program applying a flow rate of 50 $mLmin^{-1}$.

	$T_{initial}$	T_{end}	Heating rate/duration	Atmosphere
Segment 1	25 °C	100 °C	15 °C min^{-1}	N_2
Segment 2	110 °C	110 °C	10 min	N_2
Segment 3	110 °C	900 °C	30 °C min^{-1}	N_2
Segment 4	900 °C	900 °C	30 min	N_2
Segment 5	900 °C	900 °C	12 min	N_2

compounds (PACs) was also investigated. A Dionex HPLC system (Thermo Fisher/USA: UV-VIS@254 nm) equipped with a 250 × 4.6 mm 5 μm particle Eclipse PAH C-18 column (Thermo scientific, Germany) and an elution gradient was used (Table 2). As a standard, the 610 PAH Calibration Mix A (16 components) from Restek (USA) was injected with a limit of detection of 10 mg L^{-1}.

Adsorption of VFAs on ACs was investigated. For this purpose, a concentration of 10 mM propionate and acetic acid (Roth, Germany) each were added to 10.0 g char L^{-1} aqueous solution. The experiment was carried out with GR, CO_2 and Com AC in 15 mL tubes (triplicate) applying a head-over-head shaker. Samples were taken after 0.5, 1, 3, 5 and 24 h to determine propionic- and acetic acid via HPLC as described previously [28]. The respective adsorption capacities of the different chars were determined using the mass balance method. The calculation was made from the mass ratios of the adsorbate before and after the adsorption test. Adsorption capacity q was calculated following equation (6).

$$q = \frac{(C_0 - C_t) \bullet V}{m} \tag{6}$$

whereby

C_0 is the initial adsorbate concentration (in solution) before the experiment and
C_t is the equilibrium concentration after the 24 h experiment.
V is the solution volume and
m is the mass of char used.

2.4. AD batch experiments

Anaerobic digestion was carried out applying different chars (CO_2 AC, GR, $ZnCl_2$ AC, Com AC) across a range of concentrations (0, 0.025, 0.05, 0.5, 1.0, 7.0, 14.0 g L^{-1}) in 120 mL small scale batch reactors (Ochs, Germany). A total of 250 mg microcrystalline cellulose (MCC, ThermoFischer, Germany) per reactor were used as a defined, standardized carbon source with a theoretical CH_4 yield of 103.73 NmL (Fig. 1). As inoculum, sewage sludge from the waste water treatment plant in Zirl, Austria (for basic parameters please refer to Ref. [28]) was used. Before use, the sludge was fouled out for 14 d at 37 °C and anaerobically diluted 1:2 for handling purposes. According to Ref. [29], the dilution of the DS should not affect the viability of the microorganisms. Controls without MCC and char were investigated to determine basal CH_4 [NmL] production from the inoculum. All experiments were performed in triplicates. The reactors were sealed with both, butyl rubber stoppers (Ochs/Germany) and aluminum caps (Ochs/Germany) and incubated for 47 d at 37 °C. After 1 h, the gas produced was removed from each bottle using a cannula to ensure that the overpressure caused by the temperature difference was released. Gas volume (manometer), gas composition (gaschromatography), pH, and volatile fatty acids (VFAs) (HPLC) were determined on days 5, 8, 12, 21, 28, 35 and 47. On each sampling day, molecular biological samples were taken for molecular analysis of methanogen abundances and stored at −21 °C. Char concentrations were applied according to calculations based on the sludge accumulated per liter influent in a WWTP. At the Zirl waste water treatment plant, 1.25 % of sludge per liter of influent water is fed into the digestion tower. If a concentration of 0.05 g L^{-1} char of influent water were added to the WWTP, this would result in 4 g L^{-1} in the digestion tower. Depending on the capacity of the WWTP and the degree of water pollution, this percentage may increase. This would result in much higher amounts of carbon being added to the AD system. Therefore, the concentrations tested in this study reflect a realistic addition level.

A manometer (GDH200-13, Greisinger, Germany) was used for determining headspace pressure at 37 °C. The actual air pressure from a nearby weather station was used as a reference (airport of Innsbruck, Austria; www.zamg.ac.at). Gas chromatography (GC) was used to analyze gas quality according to Ref. [30]. Headspace pressure and gas concentrations were used to calculate gas production within bioreactors according to Ref. [30]. Volatile fatty acids were quantified via HPLC according to the method described by Ref. [28] using 1 mL of centrifuged and filtered (0.2 μm RC) digester content. The pH of the batch reactors was tested using pH indicator strips 5.0–10.0 (Merck, Germany).

Samples for DNA-based analysis were chosen based on CH_4 production rate. DNA was extracted from sludge samples of reactors with 1.0, 7.0, and 14.0 g L^{-1} char addition on days 12, 28 and 47. DNA was extracted using the NucleoSpin SoilExtract kit (Macherey&Nagel, Germany) according to manufacturer's protocol applying 0.9 mL of sludge sample. An elution volume of 50 μL was selected and DNA extracts were checked spectrophotometrically (Thermo Scientific Fisher, Germany). Extracts were stored in low binding tubes (Eppendorf, Germany) at −20 °C until further analysis.

Table 2
Gradient elution program for the quantification of polycyclic aromatic compounds (PACs). Solvent A: 0.1 % trifluoroacetic acid (TFA) aqueous, solvent B: 0.1 % TFA in acetonitrile.

Time [min]	Flow rate [mL min^{-1}]	Solvent A [%]	Solvent B [%]	ramp rate [% min^{-1}]
0.0	2.0	60	40	5
4.0	2.0	60	40	5
24.0	2.0	0	100	5
29.0	2.0	0	100	5
31.0	2.0	60	40	5
34.0	2.0	60	40	5

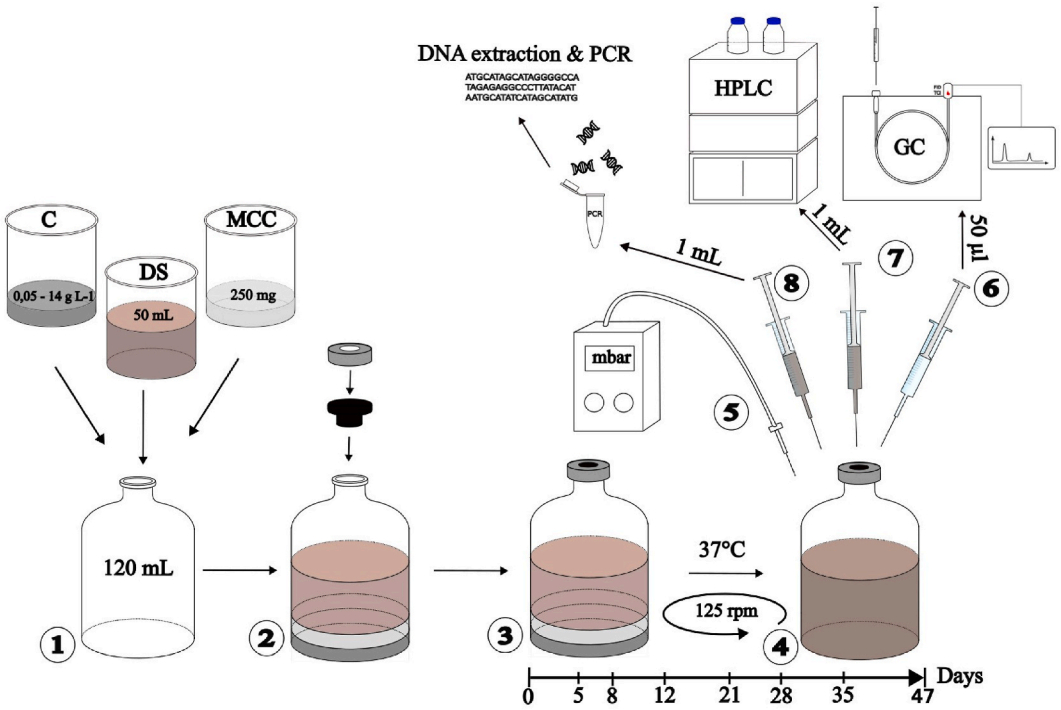

Fig. 1. Schematic of the anaerobic digestion batch test methodology. (C = char, DS = digester sludge, MCC = microcrystalline cellulose, GC = gas chromatography, HPLC = High performance liquid chromatography).

To determine the abundance of methanogens in the mini-batch reactors, qPCR was used with specific primers targeting the subunit of the methyl-coenzyme M reductase gene (*mcrA*) applying primer mlas-fwd and mcrA-rev according to Ref. [31]. Luna® Universal qPCR Master Mix was used for qPCR according to the manufacturer's instructions (NEB, Germany). Amplification was performed in a total volume of 20 µL, consisting of 18 µL diluted master mix and 2 µL of DNA template. Prior to qPCR analysis using a Rotor-Gene Q real-time PCR system (Qiagen, Germany), template DNA was diluted to 5 ng/µL. After an initial denaturation step at 95 °C, qPCR amplification was carried out over 45 cycles, each consisting of 20 s at 95 °C for denaturation and 30 s at 60 °C for annealing and elongation, respectively. After amplification, PCR products were checked by melting curve analysis (60–95 °C).

2.5. Statistical analysis

R 4.2.2 was used for statistical analysis and visualizations ("ggplot2" [32]; "tidyverse" [33]). A confidence interval of 95 % ($\alpha = 0.05$) was chosen for all statistical analyses. ANOVA was used to test the effect of char and concentration on VFA concentrations, cumulative CH_4 yield and $\log^{10}$-transformed gene copy numbers obtained from qPCR. Homogeneity of variances was checked using Levene's test (package "carData" [34]). Tukey's HSD post-hoc test (package "stats" [35]) was used for pairwise comparisons. Pearson correlation analysis were performed on char and AD properties using the package "dplyr" [36]. The R package "growthrates" [36] was used to statistically and graphically assess the growth kinetics of CH_4 production. The package includes a non-linear parametric growth model with the command "*fit_growthmodell*" and the function "*growth_logistics*", which corresponds to logistic regression. Typically, assuming that CH_4 production is equivalent to bacterial growth, the cumulative CH_4 production data were fitted to the Gomperz model. This approach has been described previously in several studies on anaerobic digestion and recommended [37].

To calculate the lag phase of each batch reactor, the time period of its linear CH_4 production was visually assessed. Within this time period, 10 time points with equal distance to each other were chosen and CH_4 production was predicted by the fitted model (command "*predict*"). Based on the predicted values, the dependency of cumulative CH_4 on time was calculated using linear regression (command "*lm*"). The lag phase of each batch experiment was defined as intersect of the predicted line with the x-axis (time).

3. Results and discussion

3.1. Characterization of the chars

In comparison to GR, the char resulting from the CO_2 post-gasification was much rougher and more porous (Fig. 3a, b). $ZnCl_2$ AC was generally less contaminated with smaller particles than the other three chars due to a washing step during the manufacturing process, and it had a highly porous structure (Fig. 3c). Except for Com AC, the wood-structures of the original material were preserved

(Fig. 3d). According to Ref. [38], this preservation of the original structure is typical for chemical ACs. In the case of Com AC (Fig. 3d), the particle size distribution was more homogeneous and the char was powdery, thereby indicating a brown or hard coal source as also supported by a high aluminum content (Table 3) [39,40]. Taken together, these results show that the properties of the char, including its porosity, were strongly influenced by the starting material and the manufacturing process.

The chars differed in their physicochemical properties (Table 3). While GR and CO_2 AC were very alkaline, Com AC was slightly above neutral, and $ZnCl_2$ AC was highly acidic. There was a positive correlation between the chars' pH and ash content. However, despite an averaged 3.56 % higher ash content than CO_2 AC, the pH-value of Com AC (Table 3) was relatively neutral at 8.62. This might be explained by low content of metal oxides, such as calcium, potassium, sodium (Table 3), and low carbon leaching (Table 4) in Com AC. Similarly, the higher ash content of CO_2 AC compared to GR was positively correlated to higher elemental concentrations (Mg, Ca, K, Na) (Table 3). Most likely, the high production temperature of 850 °C was responsible for the higher ash content of CO_2 AC [41,42]. This reasoning is supported by the undetectable low ash content of $ZnCl_2$ AC (Table 3), which had the lowest pH (2.85) of all chars tested here. The reason for this low pH is probably that basic components such as minerals and ash were selectively removed by a washing step in the manufacturing process, that is necessary to secure product quality. Given that Zn ions should display a neutral pH in aqueous solutions, the acidification may be ascribed to the washing step of the AC with an acidic solvent. This procedure results in ash components being leached, causing the carbon to become neutral. Nevertheless, the usage of the acidic solvent induced acidification of the AC.

GR had the highest carbon content at 82.66 % (Table 3), which can be explained by the progressing of the thermochemical transformation during manufacturing. The $ZnCl_2$ AC and Com AC samples had similar values of fixed carbon, with the $ZnCl_2$ AC at 80.79 ± 1.41 % and the Com AC at 79.68 ± 0.01 %. However, the $ZnCl_2$ AC had the highest volatile content of all four chars at almost 20 %. This was possibly due to the fact that $ZnCl_2$ activated samples contained more surface functional groups during the activation process, which can be detected as volatiles during thermogravimetric analysis [43]. Additionally, the higher volatile content of the starting material may have contributed to this observed phenomenon (Table 3). The Boudouard reaction has been examined due to the lower fixed carbon content of CO_2 AC compared to its precursor GR. This reaction involves the conversion of carbon into carbon monoxide utilizing CO_2 at elevated temperatures which results in the removal of carbon atoms from a char. A loss of carbon should lead to a higher mesoporosity as the pores become wider [38]. However, the nitrogen gas adsorption isotherms (Table 5) did not confirm this as both, macro- and micropores, increased after gasification, whereas mesopores decreased. Activation with $ZnCl_2$ resulted in a high proportion of micropores of about 50 %, which led to higher total pore content, although its mesopore percentages were low. Comparing all chars studied here, Com AC exhibited the highest percentages of micro- and macropores and the lowest percentage of mesopores.

As a measure of reduced carbon availability, the COD and BOD of the chars and their leachates were measured. There was no difference in COD between GR and Com AC (Table 6). Notably, BOD (in the leachate) was detectable in both chars, despite their high levels of fixed carbon, thereby suggesting that the chars might serve as a source of reduced carbon for microorganisms. Usually, char carbon occurs in a solid, chemically bound form; it is not directly available to microorganisms. The metabolization of char carbon by bacteria under aerobic conditions has been reported [66]. Therefore, char carbon forms and contents might influence the AD process. However, the BOD of GR was lower than Com AC. The COD leaching results show that all the chars, except GR, had a low release of oxidizable compounds (Table 6). For $ZnCl_2$, the low COD value was to be expected as compounds were washed out in the acidic washing step. The relatively low COD of CO_2 AC leachates, which contained GR (exhibiting a higher COD) as a feedstock, were probably due to the fact that the post-gasification had resulted in compounds that cannot be further oxidized. This was also found previously [67] reporting that biochar produced at higher temperatures had lower DOC release in aqueous environments. Generally,

Table 3
pH, electrical conductivity (EC), elemental composition and thermogravimetric analysis (TGA) of gasification residues (GR), CO_2 activated carbon (CO_2 AC), $ZnCl_2$ activated carbon ($ZnCl_2$ AC) and commercially available activated carbon (Com AC) at 1.0 g L^{-1}.

	GR	CO_2 AC	$ZnCl_2$ AC	Com AC
pH_{char}	10.74	12.63	2.85	8.62
EC_{char} (μS cm−1)	1777	16240	1456	130.6
Elemental composition				
Al/mgL^{-1}	2.54	1.79	0.43	11.84
Ca/mgL^{-1}	42.44	59.39	0.48	1.86
Fe/mgL^{-1}	1.70	2.50	0.30	7.30
K/mgL^{-1}	13.54	27.45	0.24	0.18
Mg/mgL^{-1}	5.05	6.24	0.15	1.11
Mn/mgL^{-1}	1.72	0.55	0.00	0.12
Na/mgL^{-1}	0.49	2.39	0.35	0.40
Ni/mgL^{-1}	0.01	0.16	0.01	0.07
P/mgL^{-1}	2.46	2.17	n.a.	0.63
S/mgL^{-1}	1.25	1.78	0.15	3.29
W/mgL^{-1}	0.00	0.00	0.55	0.00
Zn/mgL^{-1}	0.35	0.08	10.80	0.05
TGA				
Volatiles (%)	7.49 ± 0.33	10.99 ± 0.33	19.30 ± 1.32	3.73 ± 0.01
Carbon content (%)	82.66 ± 1.10	75.98 ± 0.04	80.79 ± 1.41	79.68 ± 0.01
Ash content (%)	9.89 ± 1.72	13.03 ± 0.37	0.00 ± 0.12	16.61 ± 0.01

Table 4
Anion and cation leaching [mg L^{-1}] (n = 3) of GR, CO_2 AC and Com AC at 14.0 g L^{-1}.

Ions	GR	CO_2 AC	$ZnCl_2$ AC	Com AC
Fluoride	0.00 ± 0.00	0.01 ± 0.00	n.a.	0.01 ± 0.01
Chloride	0.56 ± 0.07	0.35 ± 0.06	n.a.	0.17 ± 0.06
Phosphate	0.33 ± 0.07	0.00 ± 0.00	n.a.	0.00 ± 0.00
Sulfate	0.05 ± 0.05	0.00 ± 0.00	n.a.	0.00 ± 0.00
Sodium	0.15 ± 0.01	0.16 ± 0.01	n.a.	0.07 ± 0.01
Potassium	7.15 ± 0.12	7.19 ± 0.13	n.a.	0.00 ± 0.00
Magnesium	0.16 ± 0.03	0.00 ± 0.00	n.a.	0.02 ± 0.01
Calcium	0.31 ± 0.13	15.72 ± 0.87	n.a.	0.21 ± 0.04

Table 5
Gas adsorption of GR, CO_2 AC, $ZnCl_2$ AC and Com AC at 1.0 g L^{-1} using Brunauer–Emmett–Teller (BET) theory analysis.

Properties	GR n = 2	CO_2 AC n = 6	$ZnCl_2$ AC n = 2	Com AC n = 5
BETSSA (m^3 g^{-1})	188.1 ± 14.44	675.3 ± 35.90	1931.8 ± 61.52	964.2 ± 32.87
*V*total (cm^3 g^{-1})	0.19 ± 0.01	0.48 ± 0.03	1.20 ± 0.06	0.59 ± 0.04
% micropores (<2 nm)	27.29 ± 0.22	47.44 ± 1.27	49.68 ± 1.88	55.43 ± 3.49
% mesopores (2–50 nm)	66.05 ± 0.18	44.48 ± 0.99	42.54 ± 2.07	33.17 ± 6.12
% macropores (>50 nm)	6.66 ± 0.04	8.08 ± 0.58	7.78 ± 0.19	11.32 ± 2.68

Table 6
Chemical oxygen demand (COD) and the biological oxygen demand (BOD) in the leachate of GR, CO_2 AC, $ZnCl_2$ AC and Com AC at a respective concentration of 14.0.g L^{-1}.

Properties	GR	CO_2 AC	$ZnCl_2$ AC	Com AC
COD_{char} g/L O_2	26.78 ± 1.81	n.a.	n.a.	28.78 ± 0.85
$COD_{leaching}$ mg/L O_2	25.30	6.90	4.31	7.24
BOD_{char} mg/L O_2	15.85 ± 0.07	n.a.	n.a.	32.00 ± 0.93

n.a: not available due to low char quantities.

several studies [68–70] showed that biochar or activated carbon reduce BOD in wastewater. It was found that biochar may not only remove BOD, but also cause leaching of organic carbon [68], which is consistent with our findings (Table 6).

An- and cation analysis showed lower leaching in Com AC compared to all other chars (Table 4). GR carbon leaching had the highest levels of chloride, phosphate, sulfate, and magnesium. In contrast, CO_2 AC had the highest calcium leaching, while in GR, calcium leaching was low (Table 4). GR was the only char from which phosphate was leached.

Adsorption capacities of chars were determined in tap and de-ionized water (DI). For CO_2 AC, an adsorption capacity of acetic acid of 1.20 ± 0.18 mg g^{-1} was found after 24 h in tap water (Fig. 4A), which was 5.4 times lower than that of GR, despite its larger specific surface area. Although only a 3.7-fold reduction was observed for CO_2 AC compared to GR, a similar trend was observed when DI water was used as leaching solvent. The highest adsorption capacity for acetic acid was shown by Com AC in DI with an adsorption capacity of 22.12 ± 7.49 mg g^{-1} (Fig. 4A). Here, an average reduction of 32.97 % in acetic acid concentration was observed in the DI water and an average reduction of 25.62 % in the tap water. Similar results were also obtained in a previous study [44].

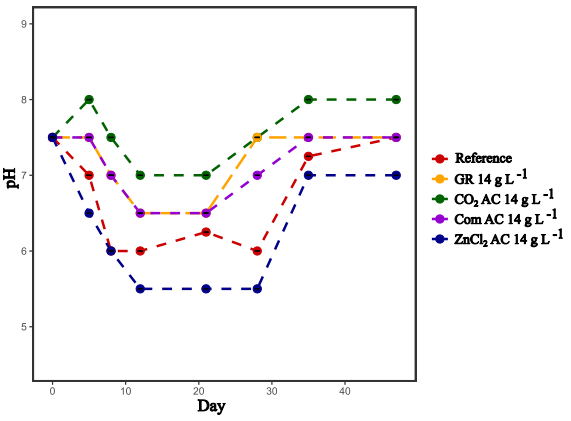

Fig. 2. pH of batch reactors over a period of 47 days with a char addition of 14.0 g L^{-1}. The concentration of 14.0 g L^{-1} was chosen exemplarily.

The adsorption capacity of propionic acid was generally higher than that of acetic acid (Fig. 4B). For Com AC, an average reduction of up to 58.80 % in DI water and 52.87 % in tap water was found. For both tested VFAs, GR had a higher adsorption capacity than CO_2 AC (Fig. 4A and B) despites the greater surface area of the latter. An average reduction in propionic acid concentration of 13.87 % in DI and 12.81 % in tap water was achieved by GR. Furthermore, all chars were found to have reduced adsorption capacity for propionic- and acetic acid in tap water compared to DI. Looking at the time course of adsoption, it is noticeable that after about 60 min desorption of both, acetic- and propionic acid, was observed for CO_2 AC (Fig. 4A and B).

3.2. Effect of char addition on AD performance

During AD, a decrease in pH was observed in all batch reactors, including the reference without char addition, probably due to VFA formation in the hydrolysis phase (Figs. 2, 7 and 8). After an initial drop of pH, being strongest for $ZnCl_2$ AC with a pH < 6 at day 10, all reactors recovered in the course of the incubation (Fig. 2). The addition of GR, CO_2 AC and Com AC resulted in higher pH values compared to the control and was probably due to an increased buffer capacity, e.g. due to higher ash content or increased concentration of inorganic materials [45]. Furthermore, char functional groups have the ability to adsorb H^+ and accept electrons, as noted in a review by Ref. [46], thereby contributing to higher buffer capacity. Methane production derived from added substrate was observed for all reactors. Theoretical CH_4 yields according to substrate's COD were not fully achieved, probably due to cellular biomass formation and other factors, such as nutrient limitation, inoculum type, and methodological variation [47].

While there was no significant effect of char type on cumulative CH_4 yield at char concentrations of 0.05, 0.15 and 0.5 g L^{-1}, at higher char concentrations (1.0, 7.0 and 14.0 g L^{-1}), differences among char types and concentrations were observed (Fig. 5). Char addition up to 1.0 g L^{-1} usually resulted in similar or higher cumulative CH_4 yields in comparison to controls. This indicates that these char concentrations tended to be neutral or slightly promoting for the reactor microbiomes substrate conversion ability. As most studies in which char was applied to AD start from 2.0 g L^{-1}, direct comparison with existing literature is hardly possible [48,49]. In contrast, Com AC at 14.0 g L^{-1} and $ZnCl_2$ AC at 7.0 and 14.0 g L^{-1} had significantly lower cumulative CH_4 yields compared to the reference. All other experiments yielded cumulative CH_4 amounts comparable to the reference (Fig. 5).

The addition of GR resulted in the highest methane yields and tended to increase the cumulative CH_4 yield at all concentrations tested (Fig. 5) as also found by Ref. [5]. With 14.0 g L^{-1} and 7.0 g L^{-1} GR addition, respectively, 7.93 % and 4.66 % more methane were produced compared to the reference. Char composition and carbon leaching (please also refer to Table 6) were likely responsible for the increased methane yields. In addition, GR also contained the highest levels of macro- and micronutrients (e.g. P and SO_2 and Ca, Mg, K, Na, Table 3), which might have been beneficial for microbial processes and activity as shown previously [50–52]. It has been suggested that GR components may serve as a substrate for methanogens [5]. Ref. [53] showed that microorganisms can attack the surface of biochar fragments, whereby the main carbon sources derived from unspecified water-soluble carbon components. The COD results of the carbon leaching (Table 6) support the assumption that water soluble organic compounds dissolved from GR. Moreover,

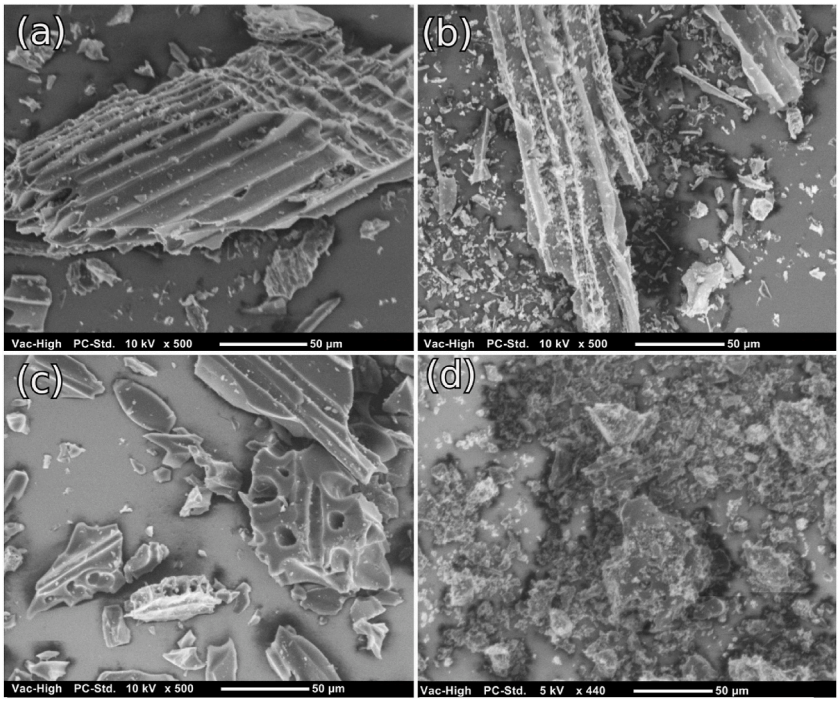

Fig. 3. The well-preserved guide vessels of the wooden feedstock of the gasification char as characterized using scanning electron microscopy (SEM): images magnified 500× of (a) GR, (b) CO_2 AC, (c) $ZnCl_2$ AC, (d) Com AC.

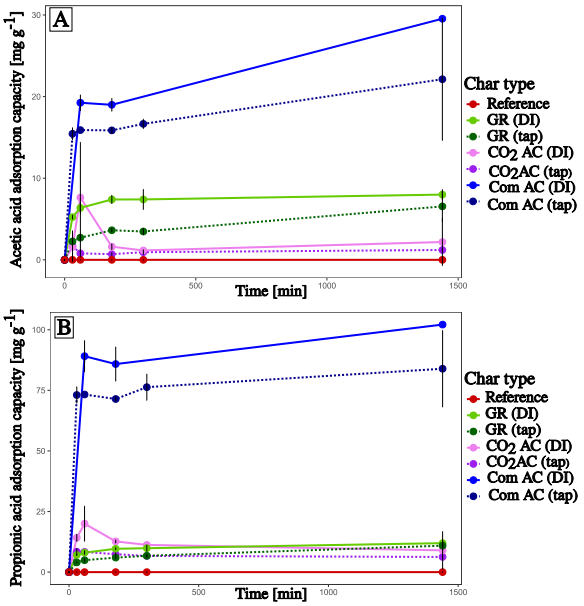

Fig. 4. Adsorption capacity for acetic acid (A) and propionic acid (B) of GR, CO_2 AC and Com AC in de-ionized water (DI water) and tap water after 30, 60, 180, 300, and 1440 min. As a reference, acetic acid and propionic acid mixture was used without the addition of GR and AC.

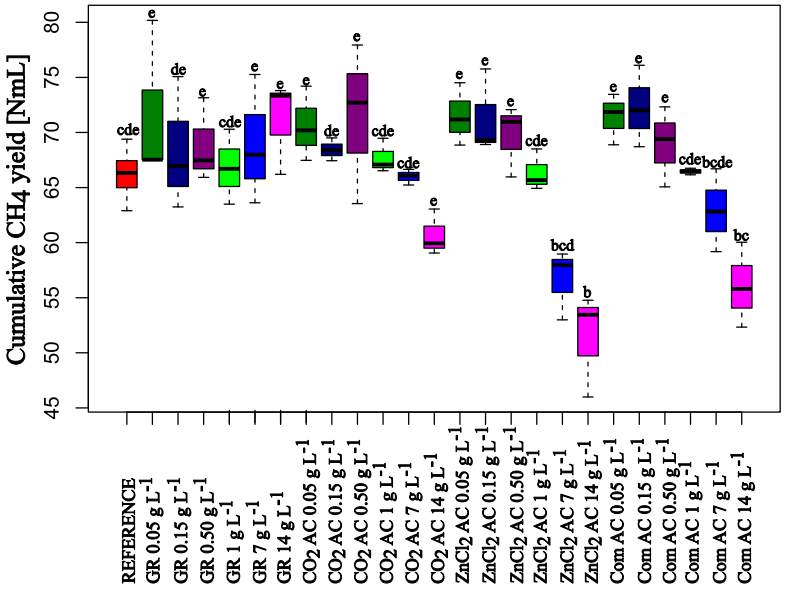

Fig. 5. Cumulative methane yields [NmL] from completed batch tests adding GR, CO_2 AC, Com AC and $ZnCl_2$ AC at 0.05, 0.15, 0.5, 1.0, 7.0 and 14.0 g L^{-1}, respectively. These results are presented in comparison with the reference condition, where no char was added.

newly discovered methoxydotrophic methanogenesis might also have been engaged in the process [54–56]. However, further molecular biological analyses are required for deeper insights. Nevertheless, the idea that GR could serve as a substrate is supported by our study.

Significantly lower cumulative CH_4 yields were found for CO_2 AC addition at a concentration of 14.0 g L^{-1}, whereas lower concentrations tended to increase methane production (Fig. 5). Similarly, Ref. [5] reported a higher CH_4 yield up to 10 g L^{-1}; a negative effect was observed at higher concentrations (34.0 g L^{-1}). Reasons for the reduced gas production might be an initially high pH of 8, especially for reactors with 14.0 g L^{-1} CO_2 AC (Fig. 2), which might have caused delayed CH_4 production (Fig. 6B and C). Leaching of

CO_2 AC introduced high Ca concentrations in the AD system (Table 4), thereby further increasing pH.

For high concentrations of Com AC, the decrease in CH_4 yield might be due to aluminum release. The toxic effect of aluminum was described previously by Ref. [57], who found that concentrations of 0.1–10.0 mg Al L^{-1} had a toxic effect on *E. coli*. Here, the high

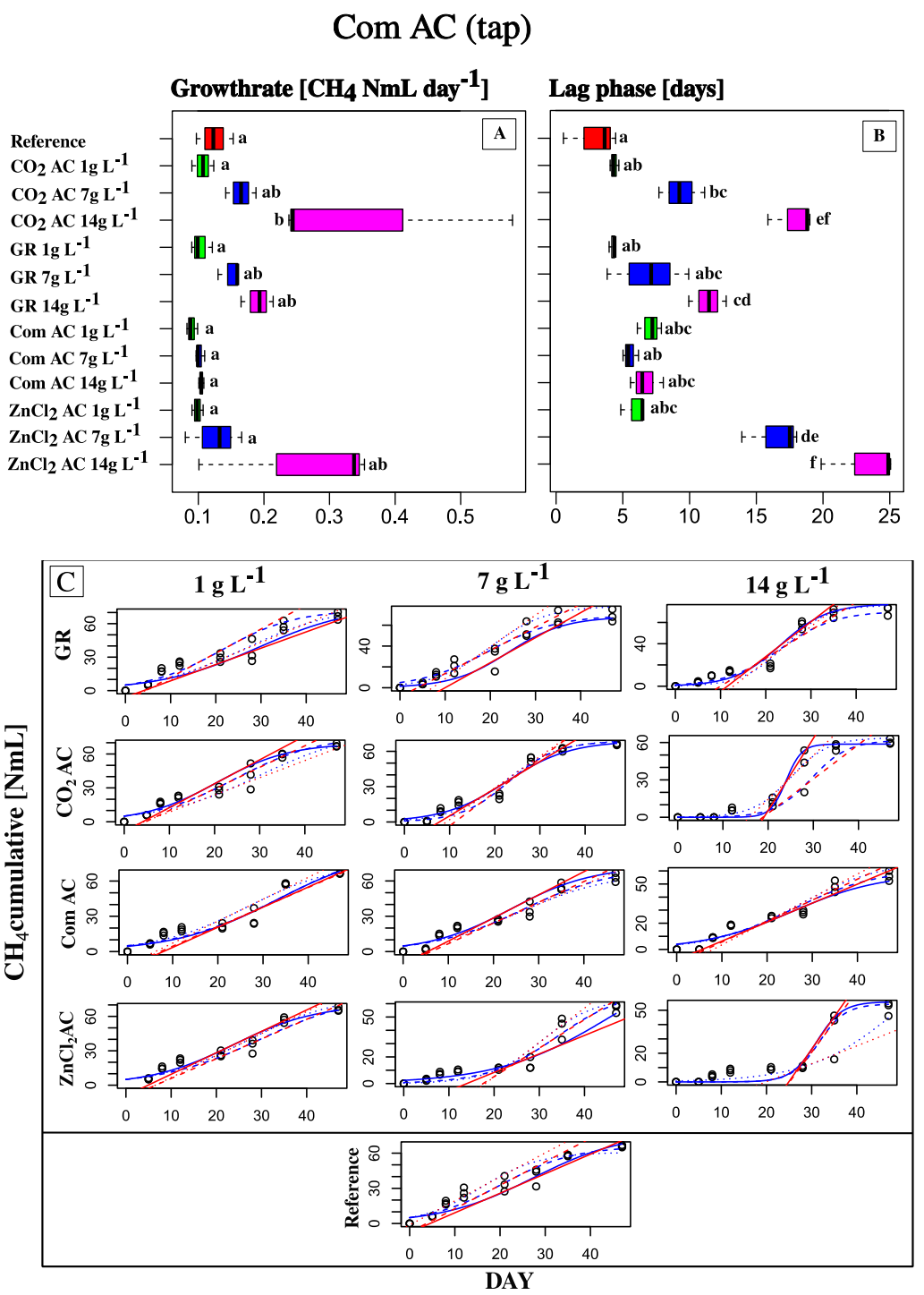

Fig. 6. Boxplot of (A) growth rate and (B) lag phase duration from cumulative CH_4 yield [NmL] of batch reactor experiment with different concentrations of GR, CO_2 AC, Com AC and $ZnCl_2$ AC. (C) Cumulative CH_4 production (points) from 47 d batch tests with logistic regression growth model (blue lines) and the linear range from the logistic regression that shows on the x-axis where methane production begins (red line). (For interpretation of the references to color in this figure legend, the reader is referred to the Web version of this article.)

concentrations of more than 10 mg L^{-1} of aluminum in Com AC (Table 3) may have inhibited bacterial growth during AD. Similar effects were found for the addition of $ZnCl_2$ AC. The high zinc leaching and content of $ZnCl_2$ AC were likely responsible for an inhibitory effect. A review by Ref. [58] reported a negative effect of zinc on AD. Conversely, zinc is an important trace element and it plays an important role in microbiological processes. A positive effect of zinc supplementation on biogas production was reported in a study by Ref. [59]. The study by Ref. [60] also confirms a beneficial effect of zinc as growth and activity of methanogenic cells was observed at a zinc concentration of up to 1.0 mg L^{-1}. It was shown that, in concentrations of up to 4.0 mg L^{-1}, zinc leads to slight inhibition, whereas stronger effects on AD were observed at 8.0 mg L^{-1} [61].

The specific surface area (SSA) of the chars was negatively correlated with cumulative CH_4 yield ($r = -0.66$, $p < 0.001$) and higher SSAs resulted in decreased methane production. In other studies, the addition of high SSA char has been found to increase methane production [62,63]. Higher SSA is thought to promote biofilm formation and thus support syntrophic interaction [64], while it may also adsorb microorganism-inhibiting substances [13]. However, further studies are needed to explain the role of SSA of different ACs in AD.

3.3. Biogas production kinetics

Biogas production kinetics were evaluated in detail for chars at concentrations of 1.0, 7.0, and 14.0 g L^{-1} (Fig. 6C) including growth rates (Fig. 6A) and lag phases (Fig. 6B); lower addition levels did not result in altered kinetics. All variants showed an initial lag phase in cumulative CH_4 production. The extent of the lag phase, however, depended on the type of char ($F(4,26) = 46.17$, $p < 0.001$) and both, char type and concentration ($F(8, 26) = 34.04$, $p < 0.001$). As observed previously for biochar [65], for all chars except Com AC, higher char concentrations prolonged the lag phase (Fig. 6B). For GR, CO_2 AC and $ZnCl_2$ AC, the lag phase was longer in comparison to the reference if added in concentrations of 7.0 and 14.0 g L^{-1}, respectively. The highest adaption time of the AD microbiome was found for $ZnCl_2$ AC (Fig. 6B). The high zinc content of 10.80 mg L^{-1} (Table 3) and the very high zinc leaching were probably responsible for this prolonged lag phase, as zinc is the second most toxic heavy metal for e.g. acetogens after copper [66].

Similar to GR and $ZnCl_2$ AC, CO_2 AC addition also prolonged the lag phase with increasing concentration compared to the reference ($p < 0.01$; Fig. 6B). This prolongation contrasts other studies reporting shorter lag phases, especially of methanogenesis [12,67] following char addition [68–70]. Using AC in AD resulted in a shortening of the lag phase for methanogenesis [12,67], in contrast to our results where all three types of activated carbon (Com AC, $ZnCl_2$ AC and CO_2 AC) resulted in a prolongation. Ref. [71] found

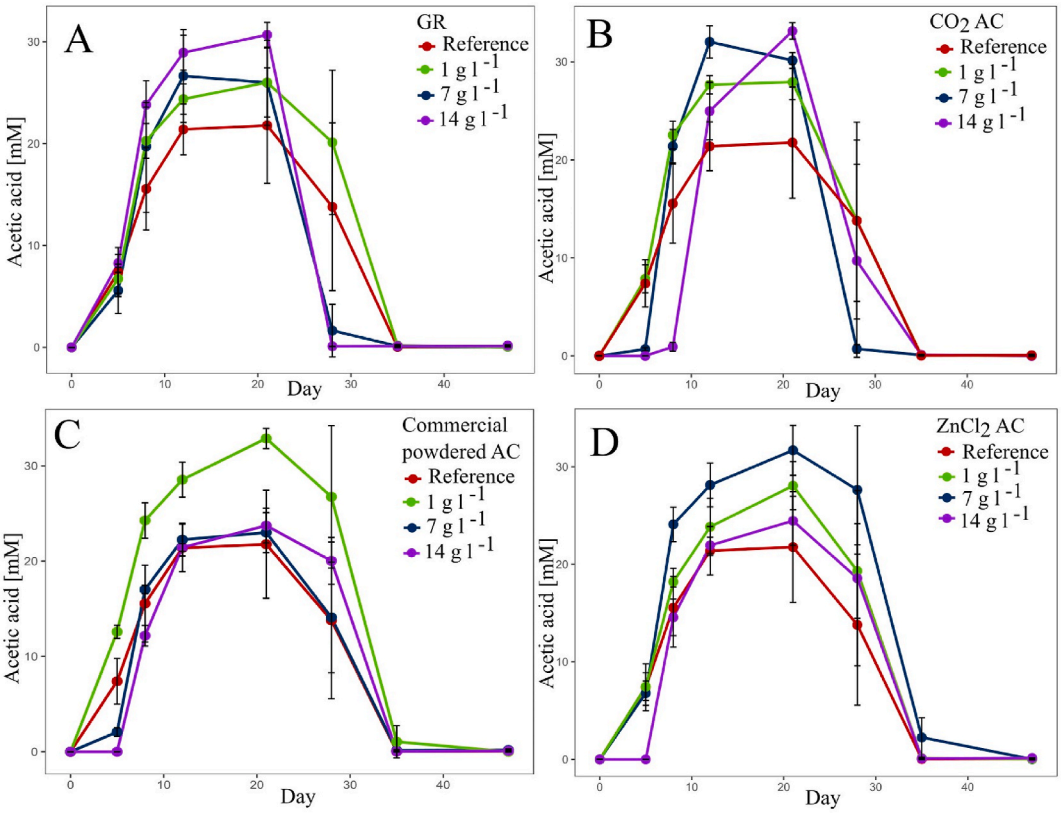

Fig. 7. Acetic acid concentration [mM] in batch reactors for different concentrations of (A) GR, (B) CO_2 AC, (C) commercial powder AC and (D) $ZnCl_2$ AC during 47 d of incubation.

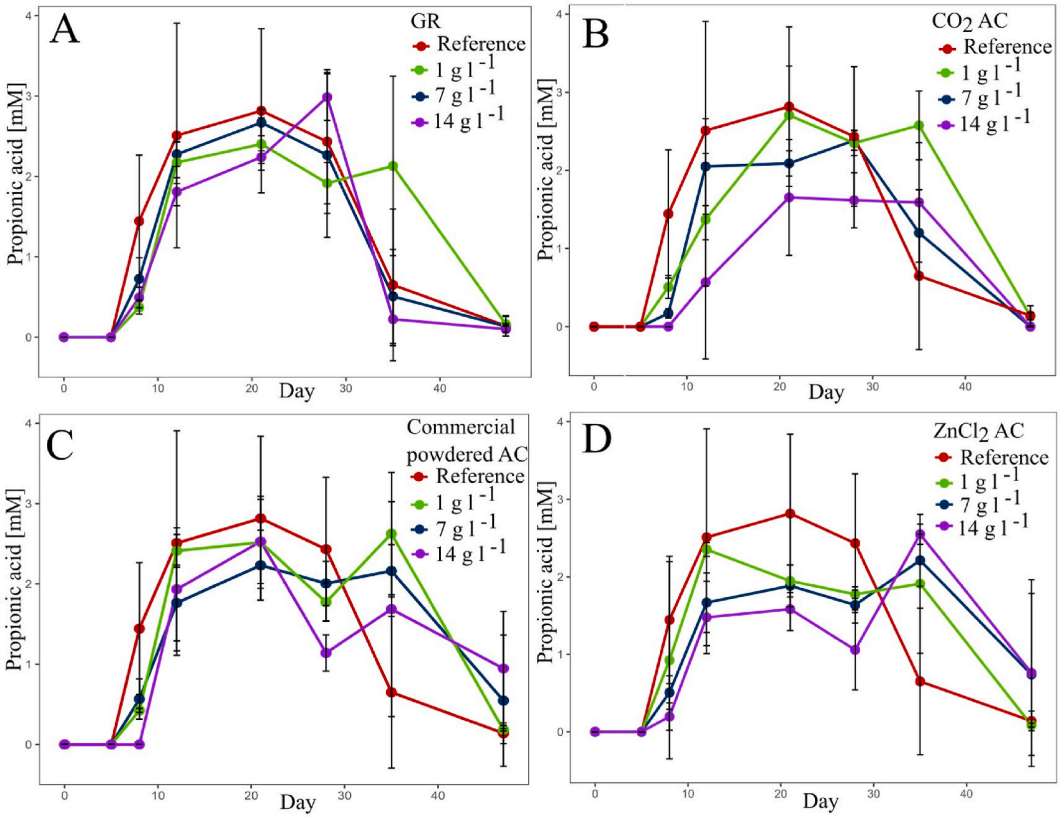

Fig. 8. Propionic acid concentration [mM] in batch reactors for different concentrations of (A) GR, (B) CO_2 AC, (C) commercial powder AC and (D) $ZnCl_2$ AC during 47 d of incubation.

reduced hydrolysis rates due to AC adsorbing the soluble substrate COD. The high adsorption capacity of char used in the present study could therefore be a reason for increased lag phases.

Correlation analysis between growth rate and lag phase duration showed a significant positive correlation ($r = 0.669$, $p < 0.001$). The growth rate was affected by the type of char ($F(4, 26 = 2.985$, $p = 0.03744$) and by both, the type of char and the char concentration ($F(8, 26 = 4.101$, $p = 0.00285$). Here, the growth rate increased with higher concentration for CO_2 AC, GR and $ZnCl_2$ AC. Due to the longer lag phase, limitations during hydrolysis have been overcome in the subsequent digestion phase as shown by the higher growth rate (Fig. 6A). This phenomenon is also known as diauxic growth, which is defined as the adaptive phase to maximise population in multi-nutrient environments.

3.4. VFAs

For all chars at an addition level of 14.0 g L^{-1}, a delay in acetic acid production was observed (Fig. 7A–D), whereas at 7.0 g L^{-1} this effect was only found for Com AC and CO_2 AC (Fig. 7A–D). The CO_2 AC and Com AC showed delayed acetic acid production in comparison to the reference already at a concentration of 7.0 g L^{-1}. However, addition of GR promoted acetic acid generation during the first phase of AD (Fig. 7A). Remarkably, higher GR concentrations stimulated microbial metabolization of acetate after 20 d of incubation, possibly by an increased addition of micro- and macronutrients (Tables 3 and 4). Similar results were also obtained for CO_2 AC (Fig. 7B).

The addition of char usually reduced the concentration of dissolved propionic acid in a concentration-affected manner during the first 28 days of incubation (Fig. 8A–D), which is in line with previous findings [72,73]. Other studies showed increased propionic acid concentrations due to biochar addition [74,75], especially during acidogenesis. A higher concentration of propionic acid was often used as an indicator of microbial stress in AD systems [76], therefore, char addition might be useful in AD processes facing limitation due to high propionic acid concentration. However, this has to be studied in detail in future investigations.

3.5. Effect of char addition on methanogenic abundance

McrA gene copy numbers were evaluated in detail for chars at concentrations of 1.0, 7.0, and 14.0 g L^{-1} (Fig. 9A–D) as lower addition levels did not affect methane production. QuantitativePCR showed significant differences in methanogen abundance between

various samples including all char types and concentrations used ($F(12, 132) = 1.91$, $p = 0.0385$; Fig. 9E and F). When compared to the reference, higher abundances of methanogens were found for all chars. There was no systematic concentration effect across chars after 47 d of incubation, where higher char addition resulted in higher *mcrA* gene copy numbers. There was a high abundance of methanogens in the inoculum, and therefore, in all reactors at the beginning of the experiment ($3.6*10^7 \pm 3.3*10^6$ copies/mL). During the first days, *mcrA* gene copy numbers decreased, but stabilized in the course of the following 47 days. In contrast to the reference, in

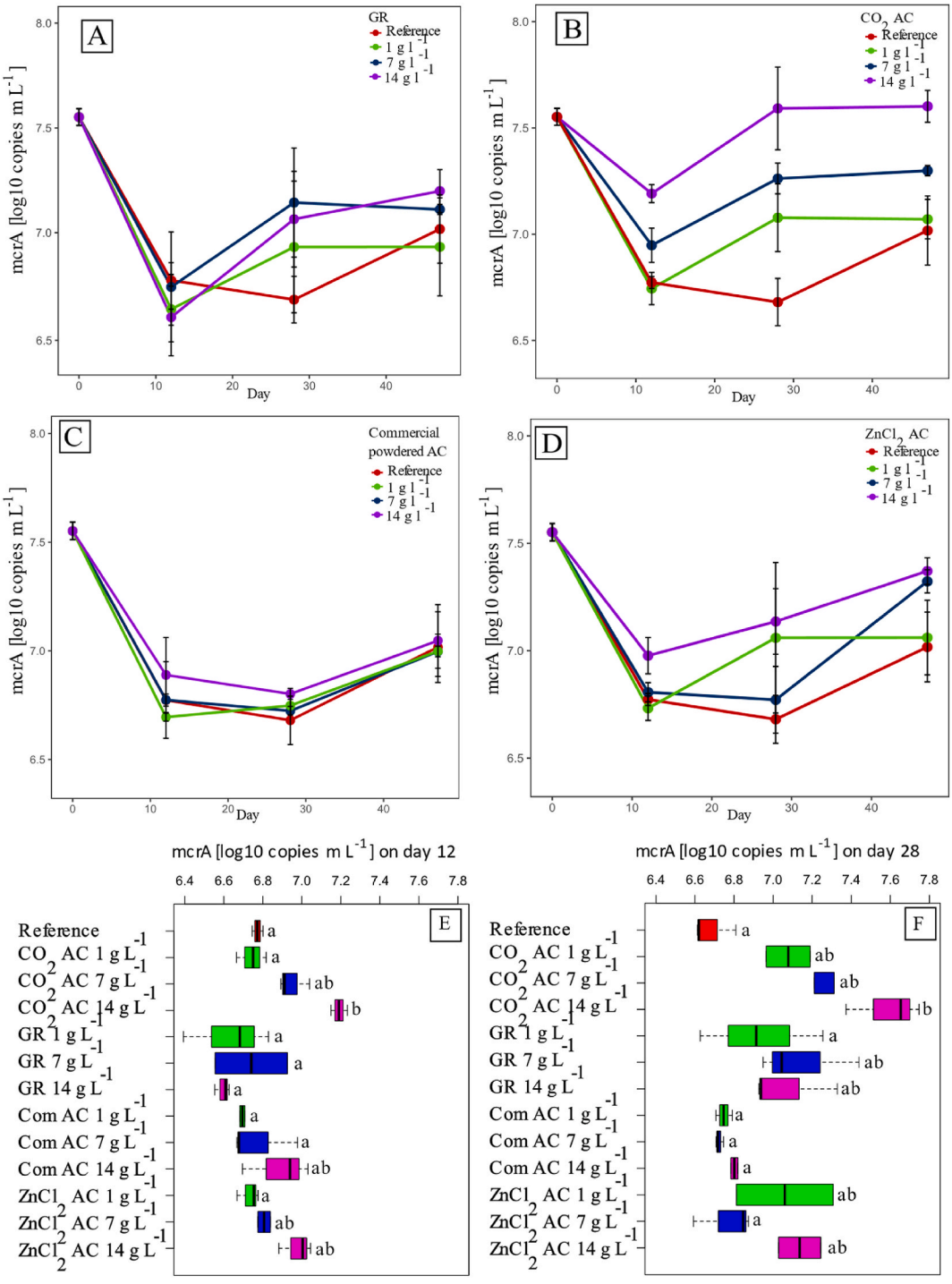

Fig. 9. *mcrA* gene abundance [log copies/mL] in the batch reactors supplemented with chars at different concentrations of 1.0, 7.0 and 14.0 g L^{-1}. (A) GR, (B) CO_2 AC, (C) commercial powder AC and (D) $ZnCl_2$ AC. (E and F) show the *mcrA* gene abundance of all chars at different concentrations from day 28 and 47, respectively.

which *mcrA* copy numbers increased after 28 days, in samples containing char (except for Com AC), the *mcrA* copy numbers started to increase after 12 days. One possible explanation for the earlier increase in methanogen abundance is the porous structure of char (Fig. 3). This provides a greater surface area for microorganisms to colonize and grow. Studies confirm that the number of methanogens increases as surface areas increase [68,77]. High surface areas may lead to biofilm formation which increases in the formation of microhabitats, in which methanogens may be protected from unfavorable conditions like very acidic pH and high antimicrobial zinc amounts ($ZnCl_2$ AC). It is important to note that, while the abundance of methanogens was higher in ZnCl2AC, the cumulative methane yield was lower compared to the reference. The observed phenomenon can be explained by the inhibition of acidogenesis caused by the extremely low pH value, as shown in the kinetics presented in Fig. 6. Possibly due to the slower supply of fatty acids, methanogens may have allocated more resources towards biomass production rather than methane production. Therefore, they may have switched to a different survival strategy because of the slower kinetics.

The buffering effect of alkaline chars might have prevented excessive acidification during acidogenesis, which is beneficial for methanogens, as they thrive optimally in a certain pH range [5,16,73,78–81]. This positive effect of char on AD is probably not only due to pH, but might also be partially ascribed to chars adding nutrients to the AD system.

Adding CO_2 AC resulted in the highest abundance of methanogens (Fig. 9B). The addition of 14.0 g L^{-1} CO_2 AC resulted in higher *mcrA* copy numbers than in the reference starting already at day 12 (day 12: $p = 0.016$; day 28: $p < 0.001$; day 47: $p < 0.001$). The high abundance of methanogens with CO_2 AC is in agreement with high growth rates (Fig. 6A), while the lower cumulative CH_4 yield with CO_2 AC addition may indicate that methanogenesis was still in progress and residual substrate was still present due to the longer lag phase (please also refer to Fig. 5).

4. Conclusions

In conclusion, this study highlights the importance of characterizing key parameters of char materials for AD. A particularly important parameter was found to be the pH of the char, which varied widely among the chars tested here. GR, with a pH of 10.7, was found to be best suited for AD, whereas zinc-activated chars exhibited an acidic pH, which inhibited methanogenic growth and/or activity. Therefore, a char's pH of at least 7 is recommended. In addition, the elemental composition of $ZnCl_2$AC with its high zinc content due to the activation method, also had a negative effect on both, AD and overall CH_4 yield. The addition of Com AC showed that parameters such as char feedstock, oxidation stage and composition can also affect both, AD and CH_4 yields. Char surface area had no significant effect on CH_4 production but did affect the relative abundance of methanogens. In particular, GR emerges as the most suitable AD additive at concentrations above 1.0 g L^{-1} leading to an average cumulative increase in CH_4 yield of 7.93 %. However, semi-continuous AD experiments are planned to improve the understanding and impact of char addition with well-characterized char.

Submission declaration

The present work has not been published previously, is not under consideration for publication elsewhere, and its publication is approved by all authors.

Data availability statement

Data will be made available on request. Data were not deposited into a publicly available repository.

Ethics declarations

This publication does not deal with human embryos and fetuses, vulnerable individuals or groups, patients, invasive techniques, personal data or sensitive personal data or dual use issues. According to the Ethics Self-Assessment of the H2020 Program, there are no ethical concerns connected to this publication.

CRediT authorship contribution statement

Christian Margreiter: Writing – original draft, Visualization, Methodology, Investigation, Formal analysis. **Maraike Probst:** Writing – review & editing, Methodology, Formal analysis, Data curation. **Eva Maria Prem:** Project administration, Methodology, Conceptualization. **Angela Hofmann:** Writing – review & editing, Validation, Supervision, Resources, Project administration, Methodology, Funding acquisition, Data curation, Conceptualization. **Andreas Otto Wagner:** Writing – review & editing, Validation, Supervision, Resources, Project administration, Methodology, Funding acquisition, Data curation, Conceptualization.

Declaration of competing interest

The authors declare that they have no known competing financial interests or personal relationships that could have appeared to influence the work reported in this paper.

Acknowledgements

Thanks to “Innsbrucker Kommunalbetriebe” and “Syncraft” for providing char and the Publikationsfonds of the Universität Innsbruck for supporting this publication. The financial support by the Austrian Federal Ministry of Labour and Economy, the National Foundation for Research, Technology and Development and the Christian Doppler Research Association is gratefully acknowledged.

Appendix A. Supplementary data

Supplementary data to this article can be found online at https://doi.org/10.1016/j.heliyon.2024.e31264.

References

[1] W. Gujer, Siedlungswasserwirtschaft: Mit 84 Tabellen. 3., Bearb. Aufl, Springer, Berlin, Heidelberg, 2007.
[2] Renewable Energy House, EBA 2018. “Statistical Report of the European Biogas Association 2018.”, 2018. Brussels, Belgium.
[3] Energie aus Biomasse: Grundlagen, Techniken und Verfahren. 3, in: M. Kaltschmitt, H. Hartmann, H. Hofbauer (Eds.), aktualisierte und erweiterte Auflage, Springer Vieweg, Berlin, Heidelberg, 2016.
[4] C. Torri, D. Fabbri, Biochar enables anaerobic digestion of aqueous phase from intermediate pyrolysis of biomass, Bioresour. Technol. 172 (2014) 335–341, https://doi.org/10.1016/j.biortech.2014.09.021 [PMID: 25277261].
[5] M. Zhang, J. Li, Y. Wang, C. Yang, Impacts of different biochar types on the anaerobic digestion of sewage sludge, RSC Adv. 9 (72) (2019) 42375–42386, https://doi.org/10.1039/C9RA08700A [PMID: 35542855].
[6] Y. Cai, M. Zhu, X. Meng, J.L. Zhou, H. Zhang, X. Shen, The role of biochar on alleviating ammonia toxicity in anaerobic digestion of nitrogen-rich wastes: a review, Bioresour. Technol. 351 (2022) 126924, https://doi.org/10.1016/j.biortech.2022.126924 [PMID: 35272033].
[7] J.-H. Park, H.-J. Kang, K.-H. Park, H.-D. Park, Direct interspecies electron transfer via conductive materials: a perspective for anaerobic digestion applications, Bioresour. Technol. 254 (2018) 300–311, https://doi.org/10.1016/j.biortech.2018.01.095 [PMID: 29398288].
[8] Y. Yan, M. Yan, G. Ravenni, I. Angelidaki, D. Fu, I.A. Fotidis, Biochar enhanced bioaugmentation provides long-term tolerance under increasing ammonia toxicity in continuous biogas reactors, Renew. Energy 195 (2022) 590–597, https://doi.org/10.1016/j.renene.2022.06.071.
[9] R.C. Bansal, M. Goyal, Activated Carbon Adsorption, Taylor & Francis, Boca Raton, 2005.
[10] C. Pan, X. Fu, W. Lu, et al., Effects of conductive carbon materials on dry anaerobic digestion of sewage sludge: process and mechanism, J. Hazard Mater. 384 (2020) 121339, https://doi.org/10.1016/j.jhazmat.2019.121339 [PMID: 31593864].
[11] S. Poirier, C. Madigou, T. Bouchez, O. Chapleur, Improving anaerobic digestion with support media: mitigation of ammonia inhibition and effect on microbial communities, Bioresour. Technol. 235 (2017) 229–239, https://doi.org/10.1016/j.biortech.2017.03.099 [PMID: 28365351].
[12] Q. Jiang, H. Liu, Y. Zhang, M.-H. Cui, B. Fu, H.-B. Liu, Insight into sludge anaerobic digestion with granular activated carbon addition: methanogenic acceleration and methane reduction relief, Bioresour. Technol. 319 (2021) 124131, https://doi.org/10.1016/j.biortech.2020.124131 [PMID: 33002784].
[13] J. Zhang, Q.W. Chua, F. Mao, et al., Effects of activated carbon on anaerobic digestion – methanogenic metabolism, mechanisms of antibiotics and antibiotic resistance genes removal, Bioresour. Technol. Rep. 5 (2019) 113–120, https://doi.org/10.1016/j.biteb.2019.01.002.
[14] L. Xiao, J. Liu, P. Senthil Kumar, M. Zhou, J. Yu, E. Lichtfouse, Enhanced methane production by granular activated carbon: a review, Fuel 320 (2022) 123903, https://doi.org/10.1016/j.fuel.2022.123903.
[15] Y. Lei, D. Sun, Y. Dang, et al., Stimulation of methanogenesis in anaerobic digesters treating leachate from a municipal solid waste incineration plant with carbon cloth, Bioresour. Technol. 222 (2016) 270–276, https://doi.org/10.1016/j.biortech.2016.10.007 [PMID: 27721101].
[16] Y. Dang, D. Sun, T.L. Woodard, L.-Y. Wang, K.P. Nevin, D.E. Holmes, Stimulation of the anaerobic digestion of the dry organic fraction of municipal solid waste (OFMSW) with carbon-based conductive materials, Bioresour. Technol. 238 (2017) 30–38, https://doi.org/10.1016/j.biortech.2017.04.021 [PMID: 28433915].
[17] Y. Zhang, Y. Cui, P. Chen, et al., Gasification technologies and their energy potentials, in: Sustainable Resource Recovery and Zero Waste Approaches, Elsevier, 2019, pp. 193–206.
[18] Y. Yan, M. Yan, G. Ravenni, I. Angelidaki, D. Fu, I.A. Fotidis, Novel bioaugmentation strategy boosted with biochar to alleviate ammonia toxicity in continuous biomethanation, Bioresour. Technol. 343 (2022) 126146, https://doi.org/10.1016/j.biortech.2021.126146 [PMID: 34673199].
[19] M. Yan, X. Zhu, L. Treu, et al., Comprehensive evaluation of different strategies to recover methanogenic performance in ammonia-stressed reactors, Bioresour. Technol. 336 (2021) 125329, https://doi.org/10.1016/j.biortech.2021.125329 [PMID: 34052546].
[20] M.N. Uddin, S.Y.A. Siddiki, M. Mofijur, et al., Prospects of bioenergy production from organic waste using anaerobic digestion technology: a mini review, Front. Energy Res. 9 (2021), https://doi.org/10.3389/fenrg.2021.627093.
[21] M. Huber, M. Huemer, A. Hofmann, S. Dumfort, Floating-fixed-bed-gasification: from vision to reality, Energy Proc. 93 (2016) 120–124, https://doi.org/10.1016/j.egypro.2016.07.159.
[22] D. Bosch, J.O. Back, D. Gurtner, S. Giberti, A. Hofmann, A. Bockreis, Alternative feedstock for the production of activated carbon with ZnCl2: forestry residue biomass and waste wood, Carbon Resources Conversion 5 (4) (2022) 299–309, https://doi.org/10.1016/j.crcon.2022.09.001.
[23] D.-W. Cho, E.E. Kwon, H. Song, Use of carbon dioxide as a reaction medium in the thermo-chemical process for the enhanced generation of syngas and tuning adsorption ability of biochar, Energy Convers. Manag. 117 (2016) 106–114, https://doi.org/10.1016/j.enconman.2016.03.027.
[24] M. Thommes, K. Kaneko, A.V. Neimark, et al., Physisorption of gases, with special reference to the evaluation of surface area and pore size distribution (IUPAC Technical Report), Pure Appl. Chem. 87 (9–10) (2015) 1051–1069, https://doi.org/10.1515/pac-2014-1117.
[25] Xylem Analytics Germany Sales GmbH & Co. KG. WTW OxiTop IS 6 Operating Manual.
[26] Product manual for Dionex IonPacTM CS12 and CG12 columns: document Nr, 034657P-05, https://tools.thermofisher.com/content/sfs/manuals/4444-Man-034657-05-IonPac-CS12-Aug05.pdf, 2005.
[27] Product manual for Dionex IonPacTH AS14A and AG14A columns: document Nr. 031678-03, Available from: URL: https://tools.thermofisher.com/content/sfs/manuals/4363-Man-031678-03-IonPac-AS14A-Nov02.pdf, 2002.
[28] A.O. Wagner, R. Markt, T. Puempel, P. Illmer, H. Insam, C. Ebner, Sample preparation, preservation, and storage for volatile fatty acid quantification in biogas plants, Eng. Life Sci. 17 (2) (2017) 132–139, https://doi.org/10.1002/elsc.201600095 [PMID: 32624760].
[29] J.J. Lay, Y.Y. Li, T. Noike, J. Endo, S. Ishimoto, Analysis of environmental factors affecting methane production from high-solids organic waste, Water Sci. Technol. 36 (6–7) (1997) 493–500, https://doi.org/10.2166/wst.1997.0628.
[30] A.O. Wagner, R. Markt, M. Mutschlechner, et al., Medium preparation for the cultivation of microorganisms under strictly anaerobic/anoxic conditions, J. Vis. Exp. 150 (2019), https://doi.org/10.3791/60155 [PMID: 31475968].
[31] L.M. Steinberg, J.M. Regan, Phylogenetic comparison of the methanogenic communities from an acidic, oligotrophic fen and an anaerobic digester treating municipal wastewater sludge, Appl. Environ. Microbiol. 74 (21) (2008) 6663–6671, https://doi.org/10.1128/AEM.00553-08 [PMID: 18776026].
[32] H. Wickham (Ed.), ggplot2, Springer International Publishing, Cham, 2016.
[33] Hadley Wickham, Mara Averick, Jennifer Bryan, et al., Welcome to the tidyverse, J. Open Source Softw. 4 (43) (2019) 1686, https://doi.org/10.21105/joss.01686.

[34] John Fox, Sanford Weisberg, Brad Price, carData: Companion to Applied Regression Data Sets, 2022. Available from: URL: https://CRAN.R-project.org/package=carData.
[35] R Core Team, R: A Language and Environment for Statistical Computing, 2022. Vienna, Austria, https://www.R-project.org/.
[36] Hadley Wickham, Romain François, Lionel Henry, Kirill Müller, Vaughan Davis, Dplyr: a grammar of data manipulation, Available from: URL: https://CRAN.R-project.org/package=dplyr, 2023.
[37] M. Dhar, P. Bhattacharya, Comparison of the logistic and the Gompertz curve under different constraints, J. Stat. Manag. Syst. 21 (7) (2018) 1189–1210, https://doi.org/10.1080/09720510.2018.1488414.
[38] P. Williams, A. Reed, Development of activated carbon pore structure via physical and chemical activation of biomass fibre waste, Biomass Bioenergy 30 (2) (2006) 144–152, https://doi.org/10.1016/j.biombioe.2005.11.006.
[39] R.A. Durie, The Science of Victorian Brown Coal: Structure, Properties and Consequences for Utilization, vol. 1, Aufl. s.l.: Elsevier Reference Monographs, 1991.
[40] B. Dai, A. Hoadley, L. Zhang, Characteristics of high temperature co-gasification and ash slagging for Victorian brown coal char and bituminous coal blends, Fuel 215 (2018) 799–812, https://doi.org/10.1016/j.fuel.2017.11.140.
[41] R.B. Fidel, D.A. Laird, M.L. Thompson, M. Lawrinenko, Characterization and quantification of biochar alkalinity, Chemosphere 167 (2017) 367–373, https://doi.org/10.1016/j.chemosphere.2016.09.151 [PMID: 27743533].
[42] J. Zhang, J. Liu, R. Liu, Effects of pyrolysis temperature and heating time on biochar obtained from the pyrolysis of straw and lignosulfonate, Bioresour. Technol. 176 (2015) 288–291, https://doi.org/10.1016/j.biortech.2014.11.011 [PMID: 25435066].
[43] K.Ö. Köse, B. Pişkin, M.K. Aydınol, Chemical and structural optimization of ZnCl2 activated carbons via high temperature CO2 treatment for EDLC applications, Int. J. Hydrogen Energy 43 (40) (2018) 18607–18616, https://doi.org/10.1016/j.ijhydene.2018.03.222.
[44] H. Wu, H. Wei, X. Yang, et al., Spherical activated carbons derived from resin-microspheres for the adsorption of acetic acid, J. Environ. Chem. Eng. 11 (2) (2023) 109394, https://doi.org/10.1016/j.jece.2023.109394.
[45] J. Zhang, W. Zhao, H. Zhang, Z. Wang, C. Fan, L. Zang, Recent achievements in enhancing anaerobic digestion with carbon- based functional materials, Bioresour. Technol. 266 (2018) 555–567, https://doi.org/10.1016/j.biortech.2018.07.076 [PMID: 30037522].
[46] M. Chiappero, O. Norouzi, M. Hu, et al., Review of biochar role as additive in anaerobic digestion processes, Renew. Sustain. Energy Rev. 131 (2020) 110037, https://doi.org/10.1016/j.rser.2020.110037.
[47] I. Angelidaki, M. Alves, D. Bolzonella, et al., Defining the biomethane potential (BMP) of solid organic wastes and energy crops: a proposed protocol for batch assays, Water Sci. Technol. 59 (5) (2009) 927–934, https://doi.org/10.2166/wst.2009.040 [PMID: 19273891].
[48] W.-X. Sun, S.-F. Fu, R. Zhu, Z.-Y. Wang, H. Zou, Y. Zheng, Improved anaerobic digestion efficiency of high-solid sewage sludge by enhanced direct interspecies electron transfer with activated carbon mediator, Bioresour. Technol. 313 (2020) 123648, https://doi.org/10.1016/j.biortech.2020.123648 [PMID: 32563791].
[49] S.-H. Lee, H.-J. Kang, T.-G. Lim, H.-D. Park, Magnetite and granular activated carbon improve methanogenesis via different metabolic routes, Fuel 281 (2020) 118768, https://doi.org/10.1016/j.fuel.2020.118768.
[50] M.S. Romero-Güiza, J. Vila, J. Mata-Alvarez, J.M. Chimenos, S. Astals, The role of additives on anaerobic digestion: a review, Renew. Sustain. Energy Rev. 58 (2016) 1486–1499, https://doi.org/10.1016/j.rser.2015.12.094.
[51] G.D. Sprott, G.B. Patel, Ammonia toxicity in pure cultures of methanogenic bacteria, Syst. Appl. Microbiol. 7 (2–3) (1986) 358–363, https://doi.org/10.1016/S0723-2020(86)80034-0.
[52] N.R. Buan, Methanogens: pushing the boundaries of biology, Emerg Top Life Sci 2 (4) (2018) 629–646, https://doi.org/10.1042/ETLS20180031 [PMID: 33525834].
[53] Y. Luo, M. Durenkamp, M de Nobili, Q. Lin, B.J. Devonshire, P.C. Brookes, Microbial biomass growth, following incorporation of biochars produced at 350 °C or 700 °C, in a silty-clay loam soil of high and low pH, Soil Biol. Biochem. 57 (2013) 513–523, https://doi.org/10.1016/j.soilbio.2012.10.033.
[54] J.M. Kurth, M.K. Nobu, H. Tamaki, et al., Methanogenic archaea use a bacteria-like methyltransferase system to demethoxylate aromatic compounds, ISME J. 15 (12) (2021) 3549–3565, https://doi.org/10.1038/s41396-021-01025-6 [PMID: 34145392].
[55] Welte CU, Revival of archaeal methane Microbiology, mSystems 3 (2) (2018), https://doi.org/10.1128/msystems.00181-17 [PMID: 29629419].
[56] D. Mayumi, H. Mochimaru, H. Tamaki, et al., Methane production from coal by a single methanogen, Science 354 (6309) (2016) 222–225, https://doi.org/10.1126/science.aaf8821 [PMID: 27738170].
[57] C.A. Jackson-Moss, J.R. Duncan, The effect of aluminium on Anaerobic digestion, Biotechnol. Lett. 13 (2) (1991) 143–148, https://doi.org/10.1007/BF01030466.
[58] C.M. Ajay, S. Mohan, P. Dinesha, M.A. Rosen, Review of impact of nanoparticle additives on anaerobic digestion and methane generation, Fuel 277 (2020) 118234, https://doi.org/10.1016/j.fuel.2020.118234.
[59] P.C. Chan, RA de Toledo, H in Iu, H. Shim, Effect of zinc supplementation on biogas production and short/long chain fatty acids accumulation during anaerobic Co-digestion of food waste and domestic wastewater, Waste Biomass Valor 10 (12) (2019) 3885–3895, https://doi.org/10.1007/s12649-018-0323-9.
[60] A. Kumar, P. Miglani, R.K. Gupta, T.K. Bhattacharya, Impact of Ni(II), Zn(II) and Cd(II) on biogassification of potato waste, J. Environ. Biol. 27 (1) (2006) 61–66 [PMID: 16850877].
[61] S.K. Jain, G.S. Gujral, N.K. Jha, P. Vasudevan, Production of biogas from Azolla pinnata R.Br and Lemna minor L.: effect of heavy metal contamination, Bioresour. Technol. 41 (3) (1992) 273–277, https://doi.org/10.1016/0960-8524(92)90013-N.
[62] M. Kumar, S. Dutta, S. You, et al., A critical review on biochar for enhancing biogas production from anaerobic digestion of food waste and sludge, J. Clean. Prod. 305 (2021) 127143, https://doi.org/10.1016/j.jclepro.2021.127143.
[63] Akturk Ali, Göksel N. Demirer, Improved food waste stabilization and valorization by anaerobic digestion through supplementation of conductive materials and trace elements, Sustainability 12 (2020) 5222.
[64] D. Zhang, W. Li, C. Hou, et al., Aerobic granulation accelerated by biochar for the treatment of refractory wastewater, Chem. Eng. J. 314 (2017) 88–97, https://doi.org/10.1016/j.cej.2016.12.128.
[65] S.O. Masebinu, O.T. Fanoro, H. Insam, et al., Can the addition of biochar improve the performance of biogas digesters operated at 45°C? Environmental Engineering Research 27 (2) (2022) 200648, https://doi.org/10.4491/eer.2020.648.
[66] C.-Y. Lin, Effect of heavy metals on acidogenesis in anaerobic digestion, Water Res. 27 (1) (1993) 147–152, https://doi.org/10.1016/0043-1354(93)90205-V.
[67] J.-H. Park, J.-H. Park, S.-H. Lee, S.P. Jung, S.-H. Kim, Enhancing anaerobic digestion for rural wastewater treatment with granular activated carbon (GAC) supplementation, Bioresour. Technol. 315 (2020) 123890, https://doi.org/10.1016/j.biortech.2020.123890 [PMID: 32731160].
[68] C. Luo, F. Lü, L. Shao, P. He, Application of eco-compatible biochar in anaerobic digestion to relieve acid stress and promote the selective colonization of functional microbes, Water Res. 68 (2015) 710–718, https://doi.org/10.1016/j.watres.2014.10.052 [PMID: 25462775].
[69] M.O. Fagbohungbe, B.M.J. Herbert, L. Hurst, H. Li, S.Q. Usmani, K.T. Semple, Impact of biochar on the anaerobic digestion of citrus peel waste, Bioresour. Technol. 216 (2016) 142–149, https://doi.org/10.1016/j.biortech.2016.04.106 [PMID: 27236401].
[70] N.M.S. Sunyoto, M. Zhu, Z. Zhang, D. Zhang, Effect of biochar addition on hydrogen and methane production in two-phase anaerobic digestion of aqueous carbohydrates food waste, Bioresour. Technol. 219 (2016) 29–36, https://doi.org/10.1016/j.biortech.2016.07.089 [PMID: 27474855].
[71] A.P. Florentino, R. Xu, L. Zhang, Y. Liu, Anaerobic digestion of blackwater assisted by granular activated carbon: from digestion inhibition to methanogenesis enhancement, Chemosphere 233 (2019) 462–471, https://doi.org/10.1016/j.chemosphere.2019.05.255 [PMID: 31181493].
[72] F. Lü, Y. Liu, L. Shao, P. He, Powdered biochar doubled microbial growth in anaerobic digestion of oil, Appl. Energy 247 (2019) 605–614, https://doi.org/10.1016/j.apenergy.2019.04.052.
[73] J. Ma, J. Pan, L. Qiu, Q. Wang, Z. Zhang, Biochar triggering multipath methanogenesis and subdued propionic acid accumulation during semi-continuous anaerobic digestion, Bioresour. Technol. 293 (2019) 122026, https://doi.org/10.1016/j.biortech.2019.122026 [PMID: 31449922].
[74] E.J. Martínez, J.G. Rosas, A. Sotres, et al., Codigestion of sludge and citrus peel wastes: evaluating the effect of biochar addition on microbial communities, Biochem. Eng. J. 137 (2018) 314–325, https://doi.org/10.1016/j.bej.2018.06.010.

[75] R. Wang, C. Li, N. Lv, et al., Deeper insights into effect of activated carbon and nano-zero-valent iron addition on acidogenesis and whole anaerobic digestion, Bioresour. Technol. 324 (2021) 124671, https://doi.org/10.1016/j.biortech.2021.124671 [PMID: 33450626].
[76] W. Gujer, A.J.B. Zehnder, Conversion processes in anaerobic digestion, Water Sci. Technol. 15 (8–9) (1983) 127–167, https://doi.org/10.2166/wst.1983.0164.
[77] P. He, H. Zhang, H. Duan, L. Shao, F. Lü, Continuity of biochar-associated biofilm in anaerobic digestion, Chem. Eng. J. 390 (2020) 124605, https://doi.org/10.1016/j.cej.2020.124605.
[78] G. Wang, Q. Li, X. Gao, X.C. Wang, Synergetic promotion of syntrophic methane production from anaerobic digestion of complex organic wastes by biochar: performance and associated mechanisms, Bioresour. Technol. 250 (2018) 812–820, https://doi.org/10.1016/j.biortech.2017.12.004 [PMID: 30001588].
[79] W. Wei, W. Guo, H.H. Ngo, et al., Enhanced high-quality biomethane production from anaerobic digestion of primary sludge by corn stover biochar, Bioresour. Technol. 306 (2020) 123159, https://doi.org/10.1016/j.biortech.2020.123159 [PMID: 32182472].
[80] L. Qiu, Y.F. Deng, F. Wang, M. Davaritouchaee, Y.Q. Yao, A review on biochar-mediated anaerobic digestion with enhanced methane recovery, Renew. Sustain. Energy Rev. 115 (2019) 109373, https://doi.org/10.1016/j.rser.2019.109373.
[81] H. Zhou, R.C. Brown, Z. Wen, Biochar as an additive in anaerobic digestion of municipal sludge: biochar properties and their effects on the digestion performance, ACS Sustainable Chem. Eng. 8 (16) (2020) 6391–6401, https://doi.org/10.1021/acssuschemeng.0c00571.